Characterization of a novel type III alcohol dehydrogenase from Thermococcus barophilus Ch5

Likui Zhang, Donghao Jiang, Yuting Li, Leilei Wu, Qing Liu, Kunming Dong, Phil M. Oger

▶ **To cite this version:**

Likui Zhang, Donghao Jiang, Yuting Li, Leilei Wu, Qing Liu, et al.. Characterization of a novel type III alcohol dehydrogenase from Thermococcus barophilus Ch5. International Journal of Biological Macromolecules, 2021. hal-03090883

HAL Id: hal-03090883
https://hal.science/hal-03090883v1

Submitted on 30 Dec 2020

HAL is a multi-disciplinary open access archive for the deposit and dissemination of scientific research documents, whether they are published or not. The documents may come from teaching and research institutions in France or abroad, or from public or private research centers.

L'archive ouverte pluridisciplinaire **HAL**, est destinée au dépôt et à la diffusion de documents scientifiques de niveau recherche, publiés ou non, émanant des établissements d'enseignement et de recherche français ou étrangers, des laboratoires publics ou privés.

Manuscript File (Word Document ONLY) Click here to view linked References

Characterization of a novel type III alcohol dehydrogenase from *Thermococcus barophilus* Ch5

Likui Zhang[1,2#], Donghao Jiang[2], Yuting Li[2], Leilei Wu[2], Qing Liu[2], Kunming Dong[2] and Philippe Oger[3#]

[1]Guangling College, Yangzhou University, China

[2]College of Environmental Science and Engineering, Marine Science & Technology Institute, Yangzhou University, China

[3]Univ Lyon, INSA de Lyon, CNRS UMR 5240, Villeurbanne, France

[#]Corresponding author: Dr. Likui Zhang

Tel: +86-514-89795882

Fax: +86-514-87357891

E-mail address: lkzhang@yzu.edu.cn

Corresponding author: Prof. Philippe Oger

E-mail address: philippe.oger@insa-lyon.fr

Abstract

The genome of the hyperthermophilic and piezophilic euryarchaeaon *Thermococcus barophilus* Ch5 encodes three putative alcohol dehydrogenases (Tba ADHs). Herein, we characterized Tba ADH_{547} biochemically and probed its mechanism by mutational studies. Our data demonstrate that Tba ADH_{547} can oxidize ethanol and reduce acetaldehyde at high temperature with the same optimal temperature (75^{o}C) and exhibit similar thermostablilty for oxidization and reduction reactions. However, Tba ADH_{547} has different optimal pH for oxidation and reduction: 8.5 for oxidation and 7.0 for reduction. Tba ADH_{547} is dependent on a divalent ion for its oxidation activity, among which Mn^{2+} is optimal. However, Tba ADH_{547} displays about 20% reduction activity without a divalent ion, and the maximal activity with Fe^{2+}. Furthermore, Tba ADH_{547} showcases a strong substrate preference for 1-butanol and 1-hexanol over ethanol and other alcohols. Similarly, Tba ADH_{547} prefers butylaldehyde to acetaldehyde as its reduction substrate. Mutational studies showed that the mutations of residues D195, H199, H262 and H234 to Ala result in the significant activity loss of Tba ADH_{547}, suggesting that residues D195, H199, H262 and H234 are responsible for catalysis. Overall, Tba ADH_{547} is a thermoactive ADH with novel biochemical characteristics, thereby allowing this enzyme to be a potential biocatalyst.

Keywords: Hyperthermophilic Archaea; Alcohol dehydrogenase; Biochemical characteristics

1 Introduction

Alcohol dehydrogenases (ADHs), which are members of the oxidoreductase family, are able to catalyze the cofactor-dependent oxidation of ethanol and other alcohols to produce the corresponding aldehydes and ketones [1]. Thus, ADHs play important roles in the detoxification and metabolism of primary and secondary alcohols. Based on their cofactor requirements, ADHs are classified into four types: nicotinamide adenine dinucleotide (NAD) dependent ADH; pyrroloquinoline quinone (PQQ) -dependent ADH; heme or cofactor F420 -dependent ADH; flavine adenine dinucleotide -(FAD) dependent ADH [2]. In addition, NAD-dependent ADHs are further subdivided into three types depending on the alcohols metabolized: short-chain ADHs exemplified by the drosophila ADH [3] (type I), medium-chain or zinc ADHs (type II or Zn-ADH) exemplified by the horse liver ADH [4], and long-chain or iron ADHs (type III or Fe-ADH) exemplified by the *Zymomonas* ADH2 [5, 6]. These three families display low similarity and arose independently throughout evolution, suggesting that these ADHs harbor different structures and mechanisms of reaction.

Several type III ADHs have been biochemically characterized since a type III ADH was first reported from *Zymomonas mobilis*, including *Saccharomyces cerevisiae* ADH4 [7], *Escherichia coli* L-1,2-propanediol oxidoreductase [8], *Clostridium acetobutylicum* ADH1 [9], *C. acetobutylicum* butanol dehydrogenases [10], and *Bacillus methanolicus* methanol dehydrogenase [11], and a human iron-activated ADH [12]. Crystal structures of the type III ADHs from bacteria and

archaea show that they possesses a very highly conserved catalytic cleft where Fe^{2+} ion is coordinated with three His residues and one Asp residue [13-16]. Currently, several type III ADHs from hyperthermophilic *Thermococcus* have been reported since the first type III ADH was characterized from *Thermococcus litoralis* [17], including *Thermococcus* strain ES-1 [18-19], *Thermococcus* strain AN1 [20], *Thermococcus hydrothermalis* [21], and *Thermococcus thioreducens* [15] and *Pyrococcus furiosus* [22]. All these reported type III ADHs from HA have one common characteristic: high thermostability, which is distinct from other ADHs from mesophiles. Although several ADHs from HA have been found, thermostable ADHs are still in demand due to unique characteristics, demonstrating a variety of substrate specificities and physiological functions.

Thermococcus barophilus Ch5, which was isolated from a deep-sea hydrothermal field of the Mid-Atlantic Ridge (Logachev field chimney, 3,020 m depth), is a thermo-piezophilic euryarchaeon, growing optimally at 88ºC under 40 MPa of hydrostatic pressure [23]. The genome of *T. barophilus* Ch5 encodes 2,679 proteins, two thirds of which have no associated functions [24]. Furthermore, several thermostable enzymes from *T. barophilus* Ch5 have been characterized [25-29] and have been shown to have distinct characteristics from other homologues found in other extremophilic archaeal models. Thus, *T. barophilus* Ch5 is an important model for studying structural and function relationship of thermostable proteins or enzymes present in hyperthermophilies as well as a great untapped source of novel extreme thermophilic enzymes for industrial processes.

Three putative alcohol dehydrogenases (Tba ADHs) are encoded in the genome of *T*. *barophilus* Ch5, including one short-chain ADH (GenBank: ALM74123) and two putative type III ADHs (GenBank: ALM74514 and ALM74601). Interestingly, these two putative Fe-ADHs from *T*. *barophilus* Ch5 have only 26% similarity in amino acid compositions, suggesting that they might harbor distinct characteristics. Currently, no ADHs from *T*. *barophilus* Ch5 has been biochemically characterized. In this work, we report the cloning, expression, biochemical characterization and mutational studies of the recombinant Tba ADH_{547} encoded by gene TBCH5v1_0547 (Genbank: ALM74514) and is conserved in all *Thermococcales* species, suggesting that this ADH might be a putative type III alcohol dehydrogenase with novel characterization.

2 Materials and methods

2.1 Materials

The pET-30a(+) vector was purchased from Novagen (Merck, Darmstadt, Germany). Plasmid Extraction Kit, PCR Cycle Pure Kit, and Gel Extraction Kit were purchased from Omega (Guangzhou, China). *Escherichia coli* DH5α cells and *E*. *coli* BL21 (DE3) cells were purchased from Transgene (Beijing, China); dNTPs, T4 DNA ligase, *Nde*I, *Xho*I, and Pfu DNA polymerase were purchased from Thermo Scientific (Waltham, MA). Chemicals were purchased from Amresco (WA, USA).

2.2 Phylogenetic analyses

The genes coding for Tba ADH_{547} and Tba ADH_{641} were used to identify their homologues in all *Thermococcales* species which genomes are sequenced. ADH

sequences were aligned in Seaview with Muscle [30]. Conserved sites were selected with GBlocks. PhyML v3.696 was employed to construct a maximum likelihood unrooted phylogenetic tree. Bootstrapping was performed with 1000 replicates. The sequence accession numbers for each individual protein is labeled in the tree. The tree was inferred with PhyML. The scale bar represents the average number of substitutions per site. Numbers at branches represent bootstrap values (1000 replicates, values > 50% are shown).

2.3 Sequence alignment

The target ADH sequences from archaea, bacteria and eukaryotes were retrieved from NCBI. The sequences were aligned by DNAMAN software version 6. The alignment figure was output with a graphic file.

2.4 Cloning of the gene encoding Tba ADH$_{547}$

We amplified the TBCH5v1_0547 gene encoding a putative type III alcohol dehydrogenase using the *T. barophilus* Ch5 genomic DNA as a template and Pfu DNA polymerase in the presence of the forward primer and the reverse primer. The sequences of these two primers are listed in Table 1. The amplified PCR product and the pET-30a(+) vector were digested by *Nde*I and *Xho*I, and the cleaved DNA fragments were ligated by T4 DNA ligase to yield the recombinant plasmid pET30a(+)-Tba ADH$_{547}$, and transformed into *E. coli* DH5α cells. After sequence verification, the recombinant plasmid pET30a(+)-Tba ADH$_{547}$ was transformed into *E. coli* BL21 (DE3) cells for expression of the Tba ADH$_{547}$ protein harboring a 6 x His-tag in its C-terminus.

2.5 Overexpression and purification of Tba ADH$_{547}$

For the Tba ADH$_{547}$ protein expression, the expression strain *E. coli* BL21 (DE3) harboring the pET30a(+)-Tba ADH$_{547}$ plasmid was cultured at 37ºC in LB medium containing 10 μg/mL kanamycin until the OD$_{600}$ reached 0.6. Then, the expression of the Tba ADH$_{547}$ gene was induced by addition of isopropyl thiogalactoside (IPTG, 0.1 mM). Expression was performed for 12 hat room temperature.

Cells were harvested by centrifugation (5,000 g) at room temperature. The collected pellet was resuspended in Ni column buffer A containing 20 mM Tris-HCl (pH 8.0), 1 mM dithiothreitol (DTT), 500 mM NaCl, 50 mM imidazole and 10% glycerol. Cells were disrupted by ultrasonication at 4ºC. Cell debris was removed by centrifugation (16,000 g) at 4ºC. The collected supernatant was heated at 70ºC for 20 min to inactivate the *E. coli* proteins. After centrifugation at 16,000 g and 4°C, the resulting supernatant was loaded onto a HisTrap FF column (GE Healthcare, Uppsala, Sweden). The Tba ADH$_{547}$ protein was eluted with NCG^{TM} Chromatography System (Bio-Rad, Hercules, CA, USA) by a linear gradient of 50–500 mM imidazole with a Ni column buffer B containing 20 mM Tris-HCl (pH 8.0), 1 mM DTT, 500 mM NaCl, 500 mM imidazole and 10% glycerol. The collected fractions containing the His-tagged Tba ADH$_{547}$ protein were analyzed by migration on a 10% SDS-PAGE. The purified Tba ADH$_{547}$ protein fractions were combined and dialyzed against a storage buffer containing 50 mM Tris-HCl (pH 8.0), 1 mM DTT, 50% glycerol and 50 mM NaCl, and stored at -80ºC. The Tba ADH$_{547}$ protein concentration was determined by measuring the absorbance at 280 nm. The theoretical molar extinction

coefficient of Tba ADH_{547} protein is predicted to be 33,350 M^{-1} cm^{-1}.

2.6 Construction, overexpression, and purification of the Tba ADH_{547} mutants

Following the manufacturer's instructions, the Tba ADH_{547} mutants were constructed by Site-Directed Mutagenesis Kit (Transgene, China) using the wild-type Tba ADH_{547} gene as a template. The sequences of the mutagenic primers are listed in Table 1. The D195A, H199A, H262A, H266A, and H274A mutant plasmids were verified by sequencing, and the mutant proteins were overexpressed, purified and quantified as described for the wild-type protein.

2.7 Enzymatic assays of Tba ADH_{547}

The standard Tba ADH_{547} enzymatic assay was performed in a total volume of 3 ml containing 100 mM Tris-HCl (pH 8.5), 0.67 mM NAD^+, 0.1 mM $MgCl_2$, 0.46 M ethanol and 500 nM Tba ADH_{547} at 75°C for 30 min and was terminated by placing samples on ice. Alternatively, the standard reaction for the reductive reaction in a total volume of 3 ml including 100 mM Tris-HCl (pH 8.5), 0.3 mM NADH, 0.46 M acetaldehyde, 0.1 mM $FeSO_4$, and 500 nM Tba ADH_{547} was conducted at 75°C for 30 min and were terminated by placing samples on ice. Tba ADH_{547} activity was determined spectrophotometrically at 340 nm by measuring the amount of NADH produced or reduced. The extinction coefficient (ε_{340}) was 6,220 M^{-1} cm^{-1}. All reactions were performed in triplicate and the average values were reported. One unit of enzyme was defined as the amount of enzyme producing or reducing 1 μmol of NADH per min.

The optimal reaction temperature of the Tba ADH_{547} activity was investigated in

the standard conditions but varying temperature in a 40ºC to 100ºC range for oxidation and in a 40ºC to 80ºC for reduction. The optimal pH of the Tba ADH_{547} activity was determined at 75°C varying the pH of the reactions between 6.5 and 10 for oxidation and between 6.0 and 8.0 for reduction. The varied pHs were adjusted with five different buffers (all at 20 mM concentrations): sodium phosphate-NaOH (pH 6.0, pH 6.5 and pH 7.0), Tris-HCl (pH 7.5, pH 8.0, and pH 8.5 at the desired temperature), and Gly-NaOH (pH 9.0, pH 9.5 and pH 10.0). The requirement for a divalent ion for the activity of Tba ADH_{547} was assayed in presence of 10 mM EDTA or 0.1 mM Fe^{2+}, Mg^{2+}, Mn^{2+}, Co^{2+}, Cu^{2+}, Ca^{2+}, Ni^{2+} or Zn^{2+}. The substrate specificity of the Tba ADH_{547} activity was investigated with ethanol, methanol, isopentanol, isopropanol, ethylene glycol, 1-butanol, 1-hexanol or glycerol as the substrates for oxidation, and with acetone, butylaldehyde, caproaldehyde or acetaldehyde as the substrates for reduction.

2.8 Kinetic assays of Tba ADH_{547}

The kinetic parameters of Tba ADH_{547} were obtained by performing reactions at different ethanol concentrations (1 mM, 5 mM, 10 mM, 20 mM, 40 mM, 80 mM, 100 mM and 200 mM) for oxidation and at different acetaldehyde concentrations (1 mM, 2.5 mM, 5 mM, 10 mM, 20 mM, 40 mM, 80 mM, and 100 mM) for reduction. The corresponding K_m and V_{max} values were calculated using the linear regression and the values given represented the calculated mean.

2.9 Circular dichroism (CD) measurements

The wild-type (WT), D195A, H199A, H262A, H266A and H274A mutant Tba

ADH_{547} proteins were dialyzed into 50 mM PBS (phosphate-buffered saline) pH7.5 for CD analysis. The CD spectra were recorded at 20°C from 200 nm to 250 nm using a J-810 spectropolarimeter (JASCO, Japan) and a cuvette of path length 0.2 cm. The spectra were generated with 0.2 mg/ml WT and mutant Tba ADH_{547} proteins at a scanning rate of 50 nm/min, and triplicate spectrum readings were collected per sample. The CD spectral data were reported as mean residue ellipticity [θ] by using the program KaleidaGraph (Synergy Software).

3 Results

3.1 Tba ADH_{547} is a putative type III alcohol dehydrogenase

Two putative NAD-ADHs of type III (Fe-ADH) are encoded in the genome of *T. barophilus* Ch5: Tba ADH_{641} and Tba ADH_{547}. As shown in Fig. 1A, Tba ADH_{547} and Tba ADH_{641} are clustered in different branches. Tba ADH_{547} is conserved in all *Thermococcales* species (Fig. 1B), including *Thermococcus*, *Pyrococcus* and *Palaeococcus* genera. Tba ADH_{547} is the most closely related to ADH from *T. paralvinellae* (Fig. 1B), and this ADH displays a relative closer relation with the ADH homologues from *Palaeococcus* than the ADH homologues from *Pyrococcus* in *Thermococcales*. Surprisingly, Tba ADH_{547} is not conserved in other Archaea (Fig. 1B). It is only distantly related to bacterial homologues (Fig. 1B). Tba ADH_{547} displays 26~30% similarity with Tba ADH_{641} and the homologues from *Thermococcus* strain ES-1, *T. hydrothermalis*, *T. litoralis*, *Thermococcus* strain AN1, *Thermococcus kodakarensis* (ADH2), *Pyrococcus furiosus*, *Z. mobilis* and *S. cerevisiae*. In contrast, Tba ADH_{547} exhibits 71~75% similarity with the homologues

from *Thermococcus* strain AN1, *T. thioreducens* and *T. kodakarensis* (ADH1), suggesting that Tba ADH_{547} might be more similar in function to *T. zilligii*, *T. thioreducens* and *T. kodakarensis* (ADH1) ADHs. Thus, the low similarity of two type III ADHs from *T. barophilus* Ch5 suggests that they might have distinct biochemical characteristics.

As shown in Fig. 2, Tba ADH_{547} possesses three conserved motifs: motif I (GGGS), motif II (DxxxH), and motif III (a conserved motif with three histidine residues), which are present in type III ADHs. However, the amino acid variations and three residues are missing in the highly conserved motif III in Tba ADH_{547} and ADHs from *T. thioreducens*, *T. kodakarensis* (ADH1) and *Thermococcus* strain AN1. Furthermore, thirty four residues are strictly conserved in all thirteen proteins (Fig. 2), including seven glycine residues, six proline residues, six alanine residues, four histidine residues, three aspartic acid residues, two lysine residues, two glutamic acid residues, one threonine, one leucine and one isoleucine. Overall, Tba ADH_{547} possesses the conserved motifs present in type III ADHs, however, displays low similarity with the homologues exemplified by Tba ADH_{641} ADH.

3.2 Cloning, expression and purification of Tba ADH_{547} protein

In this work, we cloned the Tba ADH_{547} gene encoded by TBCH5v1_0547 (Genbank: ALM74514) into a pET30a(+) expression vector and overexpressed it in *E. coli* BL21 (DE3) cells. As shown in Fig. 3A, the gene encoding the Tba ADH_{547} protein was successfully induced after addition of IPTG and the expressed protein was recovered in the supernatant after ultrasonication disruption. After heat treatment at

70°C for 30 min, most of *E. coli* proteins were inactivated and removed after centrifuge, however, the Tba ADH_{547} protein can withstand this heat treatment. Last, the recombinant Tba ADH_{547} protein was purified to near homogeneity after Ni-column affinity purification (Fig. 3A). The purified 6 x His-tagged protein displayed an approximate MW of 42 kDa (Fig. 3A), consistent with the deduced amino acid sequence.

3.3 Effect of temperature on Tba ADH_{547} activity

Since *T. barophilus* Ch5 is a hyperthermophile [23], we expect its proteins or enzymes to be highly thermophilic and thermostable. We first investigated the thermophilicity of Tba ADH_{547} by performing enzyme activity assays at varied temperatures ranging from 40°C to 100°C. As shown in Fig. 3B, Tba ADH_{547} only retained about 10% and 30% relative activity at 40°C and 100°C, respectively. Tba ADH_{547} displayed maximal activity at 75°C, which makes it a thermophilic enzyme.

Next, we determined whether Tba ADH_{547} has reduction activity. Using acetaldehyde as the substrate, we performed the reduction reaction catalyzed by Tba ADH_{547} in the presence of NADH at various temperatures ranging from 40°C to 80°C since NADH is unstable at temperatures higher than 80°C. We found that Tba ADH_{547} has the reduction activity, and also displays maximal activity for acetaldehyde reduction at 75°C (Fig. 3B). Thus, Tba ADH_{547} has the same optimal reaction temperature for both ethanol oxidation and acetaldehyde reduction under our standard reaction conditions.

3.4 Thermostablilty of Tba ADH_{547}

To probe the thermostability of Tba ADH_{547}, we incubated this ADH at varied temperatures for different times and then used the heated enzyme to perform the ethanol oxidation and acetaldehyde reduction reactions. We selected the heated Tba ADH_{547} at 90, 95 and 100^{o}C for 30 min for analyzing its reduction activity. As shown in Fig. 4A, the reduction activity of Tba ADH_{547} decreased as the heating temperature increased. However, this ADH still retained 20% reduction activity even after this ADH was heated at 100^{o}C for 30 min.

On the other hand, we employed the heated Tba ADH_{547} at 100^{o}C at varied times to analyze its oxidation reaction. Compared with the control reaction without the heating treatment, the oxidation activity of Tba ADH_{547} was lowered as the heating time extended, (Fig. 4B). However, Tba ADH_{547} still harbored about 20% oxidation activity after heating at 100^{o}C for 30 min, which is consistent with the observation for the reduction activity of the enzyme heated at 100^{o}C for 30 min. Overall, Tba ADH_{547} is a thermophilic and thermostable ADH, suggesting it potential application in ethanol oxidation and acetaldehyde reduction at high temperature.

3.5 Effect of pH on Tba ADH_{547} activity

Next, we investigated the optimal pH for ethanol oxidation and acetaldehyde reduction of Tba ADH_{547}. As shown in Fig. 5A, no Tba ADH_{547} activity was observed below pH 6.5 and only a residual activity was detected at pH 10. Tba ADH_{547} can oxidize ethanol in the pH range from 7.0 to 10.0. At pH 8.5, Tba ADH_{547} displayed maximal activity, suggesting that pH 8.5 is the optimal pH for the reduction reaction of this ADH.

The effect of pH on reduction reaction of Tba ADH_{547} was also determined using varied pH buffers ranging from 6.0 to 8.0 since NADH is unstable at above pH 8.0 (Fig. 5A). Tba ADH_{547} exhibited maximal reduction activity at pH7.0, suggesting that its optimal reaction pH is 7.0, which is lower than that of its oxidation reaction. Thus, Tba ADH_{547} displays distinct optimal pH adaptation for oxidation and reduction reactions.

3.6 Effect of divalent ions on Tba ADH_{547} activity

The metal requirements of archaeal NAD-dependent ADHs are very variable, thus, we investigated the metal dependency of Tba ADH_{547} activity for ethanol oxidation. In the absence of the addition of a divalent ion or in the presence of 10 mM EDTA (the latter should chelate the divalent ions eventually co-purified with the Tba ADH_{547} enzyme), Tba ADH_{547} yielded no measurable activity (Fig. 5B). The activity in Tba ADH_{547} is restored to some extent upon addition of all the divalent ions tested. Maximum Tba ADH_{547} activity was observed in the presence of 0.1 mM Mn^{2+}. By contrast, the lowest activity of Tba ADH_{547} was found in the presence of 0.1 mM Zn^{2+}, Cu^{2+}, Ca^{2+}, Ni^{2+}, Co^{2+}, Mg^{2+} or Fe^{2+}, which stimulated Tba ADH_{547} activity with less than 50% of that observed with Mn^{2+}. Thus, Tba ADH_{547} is dependent on a divalent ion for ethanol oxidation, which is sharply contrasted to the currently reported ADHs.

Compared with the oxidation reaction, Tba ADH_{547} displays about 30% reduction activity in the absence of divalent ion or in the presence of EDTA (Fig. 5B). Surprisingly, this ADH exhibits maximal reduction activity in the presence of Fe^{2+}, suggesting that Fe^{2+} is the optimal divalent ion for its reduction activity, which is

sharply contrasted with the observation that Mn^{2+} is the optimal ion for the oxidation activity of this ADH. Compared with the control reactions without divalent ion or without EDTA, Ca^{2+} slightly inhibited the reduction activity whereas Cu^{2+}, Mg^{2+}, or Ni^{2+} stimulated the reduction activity of this ADH with varied degrees. On the other hand, Zn^{2+} or Mn^{2+} enables this ADH to retain similar reduction activity to the control reactions. Thus, Tba ADH_{547} displays distinct divalent ion adaptation for acetaldehyde reduction.

3.7 Substrate specificity of Tba ADH_{547}

We determined the substrate specificity of Tba ADH_{547} under the optimal conditions (75°C, pH 8.5 and 0.1 mM Mn^{2+}) for oxidation. Quite strikingly, we found that the recombinant Tba ADH_{547} exhibited the highest activity in the presence of 1-butanol or 1-hexanol and not in the presence of ethanol, suggesting that 1-butanol and 1-hexanol are more suitable substrates for this enzyme than is ethanol (Fig. 6A). Only a few other primary alcohols were possible substrates for Tba ADH_{547}, including ethylene glycol (40% activity), isopentanol (25% activity), isopropanol (10% activity) and glycerol (5% activity). In contrast, we observed that Tba ADH_{547} is fully inactive on methanol. Thus, Tba ADH_{547} displays a preference for substrate in the order from high to low: 1-butanol > 1-hexanol > ethanol > ethylene glycol > isopentanol > isopropanol > glycerol. Combining all these observations, we can conclude that the optimal reaction conditions for Tba ADH_{547} activity with 1-butanol as a substrate are: 75°C, pH 8.5 and 0.1 mM Mn^{2+}. Under the optimal reaction conditions, we measured the specific activity of Tba ADH_{547} to be 931 U/mg for 1-butanol oxidation.

Next, we determined the substrate specificity of reduction reaction of Tba ADH_{547} using acetone, acetaldehyde, caproaldehyde and butylaldehyde as the substrates. Similar to the oxidation reaction with 1-butanol as a preference substrate, Tba ADH_{547} displayed higher reduction activity in the presence of butylaldehyde than in the presence of acetaldehyde (Fig. 6B), suggesting that butylaldehyde is more suitable substrate than acetaldehyde for reduction reaction of this ADH. Compared with the acetaldehyde reduction reaction, Tba ADH_{547} retained significantly lowered reduction activity for acetone and caproaldehyde reduction, suggesting that acetone and caproaldehyde are also possible substrates for reduction activity of this ADH. Thus, the optimal reaction conditions for Tba ADH_{547} reduction activity with butylaldehyde as a substrate are: 75^{o}C, pH 7.0 and 0.1 mM Fe^{2+}. The specific activity of Tba ADH_{547} was measured to be 3924 U/mg for butylaldehyde reduction, suggesting that this ADH has a higher activity for aldehyde reduction than alcohol oxidation.

3.8 K_m and V_{max} for Tba ADH_{547}

We determined the kinetic parameters of Tba ADH_{547} using the ethanol at varied concentrations ranging from 1 mM to 200 mM as the substrates under the optimal oxidation conditions as described above. The K_m and V_{max} values were calculated to be 92 mM and 8 x 10^{-3} mM/min from the fitted Lineweaver-Burk plot (Fig. 7A), respectively. Considering that 500 nM Tba ADH_{547} was employed in oxidation reaction, the K_{cat} was further measured to be 0.27 s^{-1}.

Furthermore, we examined the kinetic parameters of Tba ADH_{547} using the

acetaldehyde at varied concentrations ranging from 1 mM to 80 mM as the substrates under the optimal reaction condition (75°C, pH 7.0 and 0.1 mM Fe^{2+}). As shown in Fig. 7B, the K_m and V_{max} values of Tba ADH_{547} for acetaldehyde reduction were estimated to be 34.5 mM and 0.266 mM/min from the fitted Lineweaver-Burk plot, respectively. The corresponding K_{cat} for acetaldehyde reduction was further calculated to be 69 s^{-1}, which is about 256-fold higher than that for ethanol oxidation. By contrast, the K_m value for acetaldehyde reduction of Tba ADH_{547} is about 2.7-fold lower than that for ethanol oxidation. Thus, Tba ADH_{547} displays higher catalytic efficiency for acetaldehyde reduction than for ethanol oxidation.

3.9 Mutational studies of Tba ADH_{547}

As shown in Fig. 2A, Tba ADH_{547} harbors three conserved motifs with several conserved amino acid residues present other ADHs. To reveal key amino acid residues for catalysis of Tba ADH_{547}, we constructed the D195A, H199A, H262A, H266A, and H274A mutants. Following the wild-type protein expression and purification, we purified five Tba ADH_{547} mutant proteins (Fig. 8A).

To investigate whether the D195A, H199A, H262A, H266A, and H274A mutants cause the overall structure change of Tba ADH_{547}, we performed the CD analysis of the WT and mutant enzymes. The D195A, H199A, H262A, H266A, and H274A mutants displayed different conformational change from the wild-type Tba ADH_{547} with varied degrees (Fig. 8B). Specifically, the D195A, H266A and H274A mutants exhibited similar overall structure (Fig. 8B), which are distinct from the WT enzyme. Furthermore, the H199A substitution caused maximal change of overall structure of

the WT enzyme, followed by three substitutions (D195A, H266A and H274A) and the H262A substitution (Fig. 8B). Thus, our observations demonstrate that the D195A, H199A, H262A, H266A, and H274A substitutions disrupt the overall structure of the WT enzyme.

Next, we investigated the ethanol oxidation and acetaldehyde reduction activities of these five mutants. Compared with the wild-type protein, the D195A mutant displayed no reduction activity and the slight weak oxidation activity (Fig. 8C), suggesting that D195 is a key residue for catalysis of this ADH. Similarly, the H262A mutant harbored the weak oxidation activity (2.9%) and reduction activity (6.4%), thereby indicating that H262 is also a key residue for catalysis. However, the H266A mutant had the higher reduction activity (134%) but the lower oxidation activity (36%) than the wild-type protein, suggesting that the mutation of H266 to Ala stimulates its reduction activity but suppresses its oxidation activity. Furthermore, the H199A and H274A mutants retained 10%~20% oxidation and reduction activity, demonstrating that residues H199 and H274 are involved partially in catalysis. Overall, residues D195 and H262 in Tba ADH_{547} are essential for catalysis, and residues H199 and H274 are also involved partially in catalysis.

4. Discussion

In this work, we present the biochemical characteristics and mutational studies of Tba ADH_{547} which is one of the ADHs of the hyperthermophilic and piezophilic euryarchaeon *T. barophilus* Ch5. Tba ADH_{547} belongs to a cluster of type III archaeal ADHs (Table 2) since this enzyme harbors three conserved motifs present in

iron-containing ADHs. However, Tba ADH_{547} displays low amino acid similarity with the reported iron-containing ADHs from hyperthermophiles, including *T. litoralis* [17], *T. hydrothermalis* [21], *Thermococcus* strain ES-1 [18], *P. furiosus* [22] and *Thermotoga hypogea* [31], suggesting this ADH might be a novel type III ADH. Comparison of biochemical characteristics of iron-containing ADHs from hyperthermophiles is summarized in Table 2, displaying distinct properties for oxidation or reduction.

As expected, Tba ADH_{547} displays maximal enzyme activity at high temperatures since it originates from the hyperthermophlilic euryarchaeon *T. barophilus* Ch5. In comparison to other thermostable type III ADHs, Tba ADH_{547} displays thermophilicity 5~10ºC degrees lower than that reported for ADHs from *T. hydrothermalis* (80°C) [21], *T. litoralis* (85°C) [17] and *Thermococcus* strain AN1 (85°C) [20]. Interestingly, the optimal temperatures of ADHs from *Thermococcus* strain ES-1, *P. furiosus* and *T. hypogea* exceeded 100°C and could not be clearly determined [18, 22, 31]. To our knowledge, we first measured the optimal temperature of acetaldehyde reduction, demonstrating the same optimal temperature for ethanol oxidation under our assay conditions. Overall, Tba ADH_{547} harbors a relatively low optimal temperature for its activity, compared with the reported type III ADHs from hyperthermopiles.

In this work, we revealed that Tba ADH_{547} retains about 40% and 20% activity after being heated at 95ºC and 100ºC for 30 min, respectively. The half-life of *P. furiosus* ADH was reported to be 7 h at 95ºC [22] while the half-life of *T. litoralis*

ADH was about 0.3 h at 95ºC [17]. *Thermococcus* strain ES-1 and *T. hypogea* ADHs retain 50% activity after being heated at 95ºC for 4 h and at 90ºC for 2 h, respectively [32, 34]. A half-life of *Thermococcus* strain AN1 ADH was measured to be only 16 min at 80°C [20]. Furthermore, *T. hydrothermalis* ADH abolishes 50% activity at 80ºC for 0.25 h [21]. Thus, the type III ADHs from hyperthermophiles exhibits strong thermostability, but their degree of thermostability varies with different their host sources.

Maximal activity of Tba ADH_{547} for ethanol oxidation was observed at pH 8.5, which is similar to other type III ADHs from *T. litoralis* and *Thermococcus* strain ES-1 [17-18]. Tba ADH_{547} differs significantly from other extremophilic type III ADHs displaying a lower pH optimum than the type III-ADHs from *T. hydrothermalis*, *P. furiosus* and *T. hypogea* [21-22, 31]. However, maximal activity of Tba ADH_{547} for acetaldehyde reduction was measured at pH 7.0, suggesting that this ADH displays various optimal pH for oxidation and reduction reactions. Similar observations are found in the reported ADHs from *Thermococcus* strain ES-1 [18], *T. hydrothermalis* [21], *P. furiosus* [22], and *T. hypogea* [31].

Although the members of the Fe-ADH family are described as iron-activated alcohol dehydrogenases, these enzymes can be activated by a range of divalent cations, including zinc, nickel, magnesium, copper, cobalt, or manganese (e.g., [32-35], besides iron. To date, divalent cations are needed for a type III ADH activity, among which Fe is essentially ADHs from *Thermococcales*. However, we found that Tba ADH_{547} is the only known example of a type III archaeal ADH that is dependent

on a divalent ion for its oxidation activity. Interestingly, this ADH displays maximal oxidation activity in the presence of added Mn^{2+}. However, Tba ADH_{547} can catalyze acetaldehyde reduction reaction in the absence of a divalent ion and displays maximal activity in the presence of Fe^{2+} for acetaldehyde reduction.

Among the characterized archaeal ADHs capable of oxidizing primary alcohols, all others isolated from *Thermococcales* species exhibit a greater preference for 1-butanol over ethanol as a substrate as observed for Tba ADH_{547}. Similar to the ADHs from *Thermococcus* strain AN1 [20], *T. litoralis* [17] and *Thermococcus* strain ES-1 [18], Tba ADH_{547} shows a higher preference for primary alcohols of longer chain such as 1-hexyl alcohols. However, AdhD from *P. furiosus* essentially cannot process ethanol and has a strong preference for 1-butanol [36], and the ADH from *T. litoralis* has a marked preference for aliphatic primary alcohols [17]. In contrast to Tba ADH_{547}, *Thermococcus sibiricus* ADH, which belongs to the short-chain ADH family, demonstrates a preference for ethanol over 1-butanol, but is most probably a secondary alcohol dehydrogenase as shown by its strong preference for 2-butanol over 1-butanol [37]. In addition, similar to the ADHs from all the *Thermococcales* species listed above, Tba ADH_{547} cannot utilize methanol as a substrate. In this respect, Tba ADH_{547} and ADHs from the other *Thermococcales* differ from the ADHs found outside the *Thermococcales* order, such as *Picrophilus torridus* ADH [38] or *Thermoplasma acidophilum* ADH [39], which retain some level of activity with methanol.

As shown in Table 2, the K_m values of Tba ADH_{547} for ethanol oxidation and

acetaldehyde reduction are higher than those of the reported ADHs from the other *Thermococcales* order. Furthermore, the K_{cat} of Tba ADH_{547} for ethanol oxidation is lower than that of the reported ADHs from the other *Thermococcales* order. However, the K_{cat} of Tba ADH_{547} for acetaldehyde reduction is maximum among the all the reported ADHs listed above. Importantly, the K_{cat}/K_m of Tba ADH_{547} for acetaldehyde reduction is 670-fold higher than that for ethanol oxidation, suggesting that this ADH displays higher catalytic efficiencies for acetaldehyde reduction than ethanol oxidation as suggested by Fernandez et al. who proposed that type III ADHs from microorganisms contributed to aldehyde detoxication rather than alcohol oxidation [40]. Similarly, 13-fold, 49-fold and 3.3-fold higher K_{cat}/K_m values for acetaldehyde reduction than ethanol oxidation are observed for the ADHs from *Thermococcus* strain ES-1, *P. furiosus* and *T. hypogea* [18, 22, 31], respectively. Thus, Tba ADH_{547} displays higher K_{cat}/K_m values for acetaldehyde reduction over ethanol oxidation than other ADHs from hyperthermoplies listed above. Since *T. barophilus* Ch5 is an anaerobic euryachaeon [23], the catalytic activity of Tba ADH_{547} for ethanol synthesis is far greater than that for ethanol oxidation, which might recover the NAD^+ required for another Entner–Doudoroff glycolytic (ED) pathway under anaerobic conditions.

Alignment of amino acid sequences from type III ADH demonstrates that they possess a conserved motif III with the three highly conserved histidine residues. Mutational studies show that the H263R, H267A and H277A mutations resulted in the *E. coli* propanediol oxidoreductase without catalytic activity [41]. Crystal structure of this enzyme shows that His26 and His277 are strictly essential metal-ion ligands, and

His267 could interact with the substrate, and therefore should be involved in catalysis, but not in metal-binding [13]. Similar to *E. coli* propanediol oxidoreductase, Tba ADH_{547} harbors the corresponding residues H262, H266 and H274 in the conserved motif III. Our mutational data show that the H262A, H266A and H274A Tba ADH_{547} mutants retain 5%, 40%, and 25% oxidation activity, respectively. Thus, these observations suggest that a combination of residues H262, H266 and H274 is essential for catalysis. Surprisingly, the mutation of H266 to Ala results in 1.4-fold increase in reduction activity while the mutations of H262 and H274 to Ala lead to 75% and 90% reduction activity loss, respectively, which might be caused by overall conformational disruption due to the H262A, H266A and H274A substitutions. To our knowledge, we first revealed the function the three highly conserved histidine residues in the motif III of type III ADH in acetaldehyde reduction using Tba ADH_{547} as a target, demonstrating that residue H262 and H274 are involved in catalyzing acetaldehyde reduction reaction.

In addition to the motif II, motif II (DxxxH) with a highly conserved His residue and an Asp residue is widely present in type III ADHs. The crystal structure of *T. thioreducens* ADH shows that the conserved residues Asp193 and His197 interact with Fe atom plus residues His260 and His272 located in the conserved motif III [15]. The conserved His residue and an Asp residue in motif II are observed in the crystal structures of other type III ADHs. However, the biochemical function of the conserved His residue and an Asp residue in motif II has not been clarified. In this work, we constructed the D195A and H199A Tba ADH_{547} mutants and investigated

their activity for ethanol oxidation and acetaldehyde reduction. Note that residues D195 and H199 are analogous to residues D193 and H197 in *T*. *thioreducens* ADH. Our observations demonstrate that the D195A mutant retains slight weak activity for ethanol oxidation, and lacks acetaldehyde reduction activity. Furthermore, the H199A mutant harbors the compromised activity. Similar to the H262A, H266A and H274A substitutions, the D195A and H199A substitutions disrupt the overall structural change, which might cause the activity loss of the wild-type Tba ADH_{547}. Thus, residues D195 and H199 in Tba ADH_{547} are responsible for catalysis and maintaining their structural roles.

5. Conclusion

Herein, we present biochemical characterization of Tba ADH_{547}, displaying same optimal temperature (75^{o}C) for oxidation and reduction activities. However, this ADH has distinct optimal pH for ethanol oxidation and acetaldehyde reduction. Interestingly, Tba ADH_{547} can catalyze ethanol oxidation with a divalent ion, which is sharply contrasted to the reported ADHs. Furthermore, Tba ADH_{547} exhibits distinct divalent ion preference: Mn^{2+} for ethanol oxidation and Fe^{2+} for acetaldehyde reduction. Primary alcohols are the favored substrates for oxidation of Tba ADH_{547}, with 1-butanol yielding the highest efficiency. Furthermore, butyaldehyde is a more suitable substrate for reduction of Tba ADH_{547} than acetaldehyde. We revealed that residue D195, H199, H262 and H234 in Tba ADH_{547} are involved in catalysis by mutational studies. Overall, our findings suggest that Tba ADH_{547} might have a biotechnological potential for the biotransformation reaction due to its unique biochemical characteristics and high activity at high temperature.

Author Contributions

LZ and PO designed experiments; DJ, YL and LW performed experiments; LZ, KD, QL and PO analyzed data; LZ, KD, QL and PO wrote and revised the paper.

Declaration of Competing Interest

All authors declare that there is no conflict of interests regarding the publication of this paper.

Funding

This work was supported by the Provincial Natural Science Foundation of Jiangsu Province (No. BK20191219 and No. BK20180940), High Level Talent Support Program of Yangzhou University and the Academic Leader of Middle and Young People of Yangzhou University Grant.

Figure legends

Fig. 1. Phylogenetic analysis of Tba ADH_{641} and Tba ADH_{547}. A. Phylogenetic tree of Tba ADH_{641} and Tba ADH_{547} among bacteria and archaea. B. Phylogenetic tree of Tba ADH_{547} among bacteria and archaea.

Fig. 2. Sequence alignment of type III ADHs from bacteria, archaea and eukaryotes. Three conserved motifs (motif I: GGGS; motif II: DxxxH; motif III: the three highly conserved histidine residues) are boxed. The consensus residues are colored. The residues for engineering Tba ADH_{547} mutants are marked by an asterisk. Tba: *Thermococcus barophilus* (GenBank: ALM74514.1 for ADH_{547} and ALM74601 for ADH_{641}); Tan: *Thermococcus* strain AN1, (GenBank: WP_010477684); Tth: *Thermococcus thioreducens* (GenBank: ASJ12775); Tko: *Thermococcus kodakarensis*

(GenBank: WP_011249959 for ADH1 and WP_083755808 for ADH2); Tpa: *Thermococcus paralvinellae* (GenBank: AHF80371); Thy: *Thermococcus hydrothermalis* (GenBank: CAA74334); Tsp: *Thermococcus* sp. (GenBank: AAB63011); Tli: *Thermococcus litoralis* (GenBank: AAB63011); Pfu: *Pyrococcus furiosus* (GenBank: WP_011011187); Zmo: *Zymomonas mobilis* (GenBank: TWE26216); Sce: *Saccharomyces cerevisiae* (GenBank: GAX68104).

Fig. 3. Tba ADH_{547} can catalyze ethanol oxidation and acetaldehyde reduction reaction at high temperature. A. Overexpression and purification of Tba ADH_{547} protein. M: protein marker. B. The optimal reaction temperature of Tba ADH_{547} activity. The ethanol oxidation reactions of Tba ADH_{547} were performed in the presence of Mn^{2+} at different temperatures at pH 8.5. The acetaldehyde reduction reactions of Tba ADH_{547} were performed in the presence of Fe^{2+} at different temperatures at pH 7.0.

Fig. 4. Thermostability of Tba ADH_{547} activity. A. The thermostability for reduction reaction catalyzed by Tba ADH_{547}. The heated Tba ADH_{547} at varied temperatures for 30 min was employed to perform the acetaldehyde reduction reactions in the presence of Fe^{2+} at 75°C at pH 7.0. CK: the reaction with the non-heated enzyme. B. The thermostability for oxidation reaction catalyzed by Tba ADH_{547}. The heated Tba ADH_{547} at 100°C for varied times was employed to perform the ethanol oxidation reactions in the presence of Mn^{2+} at 75°C at pH 8.5. CK: the reaction with the non-heated enzyme.

Fig. 5. Effects pH and divalent metal ions on Tba ADH_{547} activity. A. Effect of pH on

Tba ADH_{547} activity. The ethanol oxidation reactions of Tba ADH_{547} were performed in the presence of Mn^{2+} at 75ºC at varied pHs. The acetaldehyde reduction reactions of Tba ADH_{547} were performed in the presence of Fe^{2+} at 75ºC at varied pHs. CK: the reaction without enzyme. B. Effects divalent metal ions on Tba ADH_{547} activity. The ethanol oxidation reactions of Tba ADH_{547} were performed in the presence of varied divalent metal ions at 75ºC at pH 8.5. The acetaldehyde reduction reactions of Tba ADH_{547} were performed in the presence of varied divalent metal ions at 75ºC at pH 7.0. CK: the reaction without enzyme. EDTA: the reaction with 10 mM EDTA.

Fig. 6. Substrate specificity of the oxidation activity and the reduction activity of Tba ADH_{547}. A. Substrate specificity of the oxidation activity of Tba ADH_{547}. The oxidation reactions of Tba ADH_{547} were performed in the presence of Mn^{2+} at 75ºC at pH 8.5 using varied alcohols as the substrates. B. Substrate specificity of the reduction activity of Tba ADH_{547}. The reduction reactions of Tba ADH_{547} were performed in the presence of Fe^{2+} at 75ºC at pH 7.0 using varied aldehydes as the substrates.

Fig. 7. The Lineweaver-Burk plots for ethanol oxidation and acetaldehyde reduction of Tba ADH_{547}. (A) The Lineweaver-Burk plot for ethanol oxidation of Tba ADH_{547}. The oxidation reactions of Tba ADH_{547} were performed in the presence of Mn^{2+} at 75ºC at pH 8.5 using ethanol with varied concentrations as the substrates. The Lineweaver-Burk curve was generated by plotting the reciprocal of each ethanol concentration as a horizontal ordinate and the reciprocal of each reaction rate as a vertical coordinate with a linear regression. (B) The Lineweaver-Burk plot for acetaldehyde reduction of Tba ADH_{547}. The reduction reactions of Tba ADH_{547} were

performed in the presence of Fe^{2+} at 75°C at pH 7.0 using acetaldehyde with varied concentrations as the substrates. The Lineweaver-Burk curve was generated by plotting the reciprocal of each acetaldehyde concentration as a horizontal ordinate and the reciprocal of each reaction rate as a vertical coordinate with a linear regression.

Fig. 8. Purification and the activity assays of the Tba ADH_{547} mutants. A. Purification of the WT, D195A, H199A, H262A, H266A and H274A mutant Tba ADH_{547} proteins. WT: wild-type; M: protein marker. B. CD analysis of the WT and mutant Tba ADH_{547} proteins. The mean residue ellipticity was recorded with different color line for the WT and mutant Tba ADH_{547} proteins as indicated by monitoring changes in secondary structure with scanning from 200nm to 250 nm. The CD spectra of the WT, D195A, H199A, H262A, H266A and H274A mutant Tba ADH_{547} proteins are colored with black, red, yellow, green, cyan and blue, respectively. C. The activity assays of the Tba ADH_{547} D195A, H199A, H262A, H266A and H274A mutants. The oxidation reactions of the Tba ADH_{547} mutants were performed in the presence of Mn^{2+} at 75°C at pH 8.5 using ethanol as the substrate. The reduction reactions of the Tba ADH_{547} mutants were performed in the presence of Fe^{2+} at 75°C at pH 7.0 using acetaldehyde as the substrate.

References

1. J.A. Littlechild, J.E. Guy, M.N. Isupov, Hyperthermophilic dehydrogenase enzymes, Biochem. Soc. Trans. 32 (2004) 255-258.
2. H. Radianingtyas, P.C. Wright, Alcohol dehydrogenases from thermophilic and hyperthermophilic archaea and bacteria, FEMS Microbiol. Rev. 27 (2003) 593-616.
3. D.R. Thatcher, The complete amino acid sequence of three alcohol dehydrogenase alleloenzymes (*Adh*-N11, *Adh*-s and *Adh*-UF) from the fruitfly *Drosophila melanogaster*, Biochem. J. 187 (1980) 875-886.
4. H. Eklund, B. Nordstro¨m, E. Zeppezauer, G. So¨derlund, I. Ohlsson, T. Boiwe, B.-O. So¨derberg, O. Tapia, C.-I. Bra¨nde´n, Å. Åkeson, Three-dimensional structure of horse liver alcohol dehydrogenase at 2.4 Å resolution, J. Mol. Biol. 102 (1976) 27-59.
5. D. Neale, R. K. Scopes, J. M. Delly, R. E. H. Wettenhall, The two alcohol dehydrogenases of *Zymomonas mobilis*: purification by differential dye ligand chromatography, molecular characterization and physiological roles, Eur. J. Biochem. 154 (1986) 119-124.
6. T. Conway, G. W. Sewell, Y. A. Osman, L. O. Ingram, Cloning and sequencing of the alcohol dehydrogenase II gene from *Zymomonas mobilis*, J. Bacteriol. 169 (1987) 2591-2597.

7. V. M. Williamson, C. E. Paquin, Homology of *Saccharomyces cerevisiae* ADH4 to an iron-activated alcohol dehydrogenase from *Zymomonas mobilis*, Mol. Gen. Genet. 209 (1987) 374-381.

8. T. Conway, L. O. Ingram, Similarity of *Escherichia coli* propanediol oxidoreductase (fucO product) and an unusual alcohol dehydrogenase from *Zymomonas mobilis* and *Saccharomyces cerevisiae*, J. Bacteriol. 171 (1989) 3754-3759.

9. J. S. Youngleson, W. A. Jones, D. T. Jones, D. R. Woods, Molecular analysis and nucleotide sequence of the adh1 gene encoding an NADPH-dependent butanol dehydrogenase in the gram-positive anaerobe *Clostridium acetobutylicum*, Gene 78 (1989) 355-364.

10. K. A. Walter, G. N. Bennett, E. T. Papoutsakis, Molecular characterization of two *Clostridium acetobutylicum* ATCC 824 butanol dehydrogenase isozyme genes, J. Bacteriol. 174 (1992) 7149-7158.

11. G. E. De Vries, N. Arfman, P. Terpstra, L. Dijkhuizen. Cloning, expression, and sequence analysis of the *Bacillus methanolicus* C1 methanol dehydrogenase gene. J. Bacteriol. 174 (1992) 5346-5353.

12. Y. Deng, Z. Wang, S. Gu, C. Ji, K. Ying, Y. Xie, Y. Mao, Cloning and characterization of a novel human alcohol dehydrogenase gene (ADHFe1), DNA Seq. 13 (2002) 301-306.

13. C. Montella, L. Bellsolell, R. Pérez-Luque, J. Badía, L. Baldoma, M. Coll, J. Aguilar, Crystal structure of an iron-dependent group III dehydrogenase that

interconverts L-lactaldehyde and L-1,2-propanediol in *Escherichia coli*. J Bacteriol. 187 (2005) 4957-4966.

14. J. Moon, H. Lee, S. Park, J. Song, M. Park, H. Park, J. Sun, J. Park, B. Kim, J. Kim, Structures of iron-dependent alcohol dehydrogenase 2 from *Zymomonas mobilis* ZM4 with and without NAD+ cofactor, J. Mol. Biol. 407 (2011) 413-424.
15. S.B. Larson, J.A. Jones, A. McPherson, The structure of an iron-containing alcohol dehydrogenase from a hyperthermophilic archaeon in two chemical states, Acta Crystallogr. F Struct. Biol. Commun. 75 (2019) 217-226.
16. R. Schwarzenbacher, F. von Delft, J. M. Canaves, L. S. Brinen, X. Dai, A. Deacon, M. et al, Crystal structure of an iron-containing 1,3-propanediol dehydrogenase (TM0920) from *Thermotoga maritime* at 1.3 Å resolution. Proteins, 54 (2004) 174–177.
17. K. Ma, F.T. Robb, M.W. Adams, Purification and characterization of NADP-specific alcohol dehydrogenase and glutamate dehydrogenase from the hyperthermophilic archaeon *Thermococcus litoralis*, Appl. Environ. Microbiol. 60 (1994) 562-568.
18. K. Ma, H.J. Loessner, J. Heider, M.K. Johnson, M.W.W. Adams, Effects of elemental sulfur on the metabolism of the deep-sea hyperthermophilic archaeon *Thermococcus* strain ES-1: characterization of a sulfur-regulated, non-heme iron alcohol dehydrogenase, J. Bacteriol. 177 (1995) 4748-4756.
19. X. Ying, A.M. Grunden, L. Nie, M.W. Adams, K. Ma, Molecular characterization of the recombinant iron-containing alcohol dehydrogenase from the

hyperthermophilic Archaeon, *Thermococcus* strain ES1, Extremophiles, 13 (2009) 299-311.

20. D. Li, K.J. Stevenson, Purification and sequence analysis of a novel NADP(H)-dependent type III alcohol dehydrogenase from *Thermococcus* strain AN1, J. Bacteriol. 179 (1997) 4433-4437.
21. E. Antoine, J.L. Rolland, J.P. Raffin, J. Dietrich, Cloning and over-expression in *Escherichia coli* of the gene encoding NADPH group III alcohol dehydrogenase from *Thermococcus hydrothermalis*. Characterization and comparison of the native and the recombinant enzymes, Eur. J. Biochem. 264 (1999) 880-889.
22. Ma K, Adams MWW (1999) An unusual oxygen-sensitive, iron and zinc-containing alcohol dehydrogenase from the hyperthermophilic archaeon *Pyrococcus furiosus*. J Bacteriol 181:1163-1170.
23. V.T. Marteinsson, J.L. Birrien, A.L. Reysenbach, M. Vernet, D. Marie, A. Gambacorta, P Messner, U.B. Sleytr, D. Prieur, *Thermococcus barophilus* sp. nov., a new barophilic and hyperthermophilic archaeon isolated under high hydrostatic pressure from a deep-sea hydrothermal vent, Int.J. Syst. Bacteriol. 49 (1999) 351-359.
24. P. Oger, T.G. Sokolova, D.A. Kozhevnikova, E.A. Taranov, P. Vannier, H.S. Lee, K.K. Kwon, S.G. Kang, J.H. Lee, E.A. Bonch-Osmolovskaya, A. V. Lebedinsky, Complete genome sequence of the hyperthermophilic and piezophilic archaeon *Thermococcus barophilus* Ch5, capable of growth at the expense of hydrogenogenesis from carbon monoxide and formate, Genome Announc. 4

(2016).

25. K.M. Kwon, S.G. Kang, T.G. Sokolova, S.S. Cho, Y.J. Kim, C.H. Kim, ST. Kwon, Characterization of a family B DNA polymerase from *Thermococcus barophilus* Ch5 and its application for long and accurate PCR, Enzyme Microb. Technol. 86 (2016) 117-126.
26. Y. Wang, L. Zhang, X. Zhu, Y. Li, H. Shi, P. Oger, Z. Yang, Biochemical characterization of a thermostable endonuclease V from the hyperthermophilic euryarchaeon *Thermococcus barophilus* Ch5, Int. J. Biol. Macromol. 117 (2018) 17-24.
27. H. Shi, Q. Gan, D. Jiang, Y. Wu, Y. Yin, H. Hou, H. Chen, Y. Xu, L. Miao, Z. Yang, P. Oger, Biochemical characterization and mutational studies of a thermostable uracil DNA glycosylase from the hyperthermophilic euryarchaeon *Thermococcus barophilus* Ch5, Int. J. Biol. Macromol. 134 (2019) 846-855.
28. H. Shi, Y. Huang, Q. Gan, M. Rui, H. Chen, C. Tu, Z. Yang, P. Oger, L. Zhang, Biochemical characterization of a thermostable DNA ligase from the hyperthermophilic euryarchaeon *Thermococcus barophilus* Ch5, Appl. Microbiol. Biotechnol. 103 (2019) 3795-3806.
29. Q. Gan, M. He, H. Shi, Z. Yang, P. Oger, L. Ran, L Zhang, Characterization of a Family IV uracil DNA glycosylase from the hyperthermophilic euryarchaeon *Thermococcus barophilus* Ch5, Int. J. Biol.Macromol. 146 (2020) 475-481.
30. M. Gouy, S. Guindon, O. Gascuel, SeaView version 4: a multiplatform graphical user interface for sequence alignment and phylogenetic tree building, Mol. Biol.

Evol. 27 (2010) 221-224.

31. X. Ying, Y. Wang, H.Badiei, V. Karanassios, K. Ma, Purification and characterization of an iron-containing alcohol dehydrogenase in extremely thermophilic bacterium *Thermotoga hypogea*, Arch. Microbiol. 187 (2007) 499-510.

32. S. Elleuche, K. Fodor, B. Klippel, H.A. von der, M. Wilmanns, G. Antranikian, Structural and biochemical characterisation of a NAD(+)-dependent alcohol dehydrogenase from Oenococcus oeni as a new model molecule for industrial biotechnology applications, Appl. Microbiol. Biotechnol. 97 (2013) 8963-8975.

33. G. Sulzenbacher, K. Alvarez, R.H. Van Den Heuvel, C, Versluis, S, Spinelli, V, Campanacci, et al. Crystal structure of *E. coli* alcohol dehydrogenase YqhD: evidence of a covalently modified NADP coenzyme, J. Mol. Biol. 342 (2004) 489-502.

34. S. Elleuche, K. Fodor, H.A. von der, B. Klippel, M. Wilmanns, G. Antranikian, Group III alcohol dehydrogenase from Pectobacterium atrosepticum: insights into enzymatic activity and organization of the metal ion-containing region, Appl. Microbiol. Biotechnol. 98 (2014) 4041-4051.

35. J. Extance, S.J. Crennell, K. Eley, R. Cripps, D.W. Hough, M.J. Danson, Structure of a bifunctional alcohol dehydrogenase involved in bioethanol generation in *Geobacillus thermoglucosidasius*, Acta Crystallogr. D Biol. Crystallogr. 69 (2013) 2104-2115.

36. R. Machielsen, A.R. Uria, S.W. Kengen, J. van der Oost, Production and

characterization of a thermostable alcohol dehydrogenase that belongs to the aldo-keto reductase superfamily, Appl. Environ. Microbiol. 72 (2006) 233-238.

37. T.N. Stekhanova, A.V. Mardanov, E.Y. Bezsudnova, V.M. Gumerov, N.V. Ravin, K.G. Skryabin, V.O. Popov, Characterization of a thermostable short-chain alcohol dehydrogenase from the hyperthermophilic archaeon *Thermococcus sibiricus*, Appl. Environ. Microbiol. 76 (2010) 4096-4098.
38. M. Hess, G. Antranikian, Archaeal alcohol dehydrogenase active at increased temperatures and in the presence of organic solvents, Appl. Microbiol. Biotechnol. 77 (2008) 1003-1013.
39. E.N. Marino-Marmolejo, A.D. León-Rodríguez, A.P.B. de la Rosa, L. Santos, Heterologous expression and characterization of an alcohol dehydrogenase from the archaeon *Thermoplasma acidophilum*, Mol. Biotechnol. 42 (2009) 61-67.
40. M.R Fernandez, J.A. Biosca, A. Norin, H. JoÃrnvall, X. PareÂs, Class III alcohol dehydrogenase from *Saccharomyces cerevisiae*: Structural and enzymatic features differ toward the human/mammalian forms in a manner consistent with functional needs in formaldehyde detoxication, FEBS Lett. 370 (1995) 23-26.
41. N. Obradors, E. Cabiscol, J. Aguilar, J. Ros, Site-directed mutagenesis studies of the metal-binding center of the iron-dependent propanediol oxidoreductase from *Escherichia coli*, Eur. J. Biochem. 258 (1998) 207-213.

Table 1 Sequences of the oligonucleotides used to clone the Tba ADH_{547} gene and construct its mutants

Name	Sequence (5′-3′)
Tba ADH_{547} F	GGGAATTC*CATATG*CAGTTCTTCAGCTTAAAGAC
Tba ADH_{547} R	CCG*CTCGAG*ATCATAGAAGGCTCTCTTATAC
D195A F	AAGGAACAGCGGACTGGCTGTTCTGGTGCAC
D195A R	GCCAGTCCGCTGTTCCTTGCAACTTCTTTTG
H199A F	GACTGGATGTTCTGGTGGCCGGAATTGAAGCT
H199A R	GCCACCAGAACATCCAGTCCGCTGTTCCTTGC
H262A F	CCCGTTTAGGCTTGTGCGCCAGCTTAAGCCAT
H262A R	GCGCACAAGCCTAAACGGGCATTAAGAAAAGC
H266A F	TGTGCCACAGCTTAAGCGCTAAAGCGGCTTGG
H266A R	GCGCTTAAGCTGTGGCACAAGCCTAAACGGGC
H274A F	CGGCTTGGATTGCCCCTGCCGGCTTGTTAAAT
H274A R	GCAGGGGCAATCCAAGCCGCTTTATGGCTTAA

The italic bases represent restriction sites.

The substitution bases are underlined.

Table 2 Comparisons of biochemical characteristics of iron-containing ADH members from hydrothermophiles.

Organism		T/°C optimum	pH optimum	K_m (mM)	K_{cat} (s^{-1})	K_{cat}/K_m ($s^{-1}M^{-1}$)	Reference
T. barophilus	Oxidation[a]	75	8.5	92	0.27	2.9	This work
	Reduction[b]	75	7.0	34.5	69	2.0×10^3	
Thermococcus strain AN1	Oxidation	85	6.8-7.0	ND	ND	ND	[20]
	Reduction	ND	7.0	0.12	ND	ND	
T. litoralis	Oxidation	85	8.8	11	26	2.3×10^3	[17]
	Reduction	ND	ND	0.4	ND	ND	
T. hydrothermalis	Oxidation	80	10.5	ND	ND	ND	[21]
	Reduction	ND	7.5	ND	ND	ND	
Thermococcus strain ES-1	Oxidation	>95	8.8-10.4	8.0	48	6.0×10^3	[18]
	Reduction	ND	ND	0.25	19	7.6×10^4	
P. furiosus	Oxidation	>95	9.4-10.2	29.4	19	6.5×10^2	[22]
	Reduction	ND	ND	0.17	5.5	3.2×10^4	
T. hypogea	Oxidation	>95	11.0	9.7	14	1.5×10^3	[31]
	Reduction	ND	8.0	3.1	15	5.0×10^3	

a: Ethanol oxidation reaction; b: Acetaldehyde reduction; ND: Not determined

Click here to access/download;Figure;Fig-1.pdf

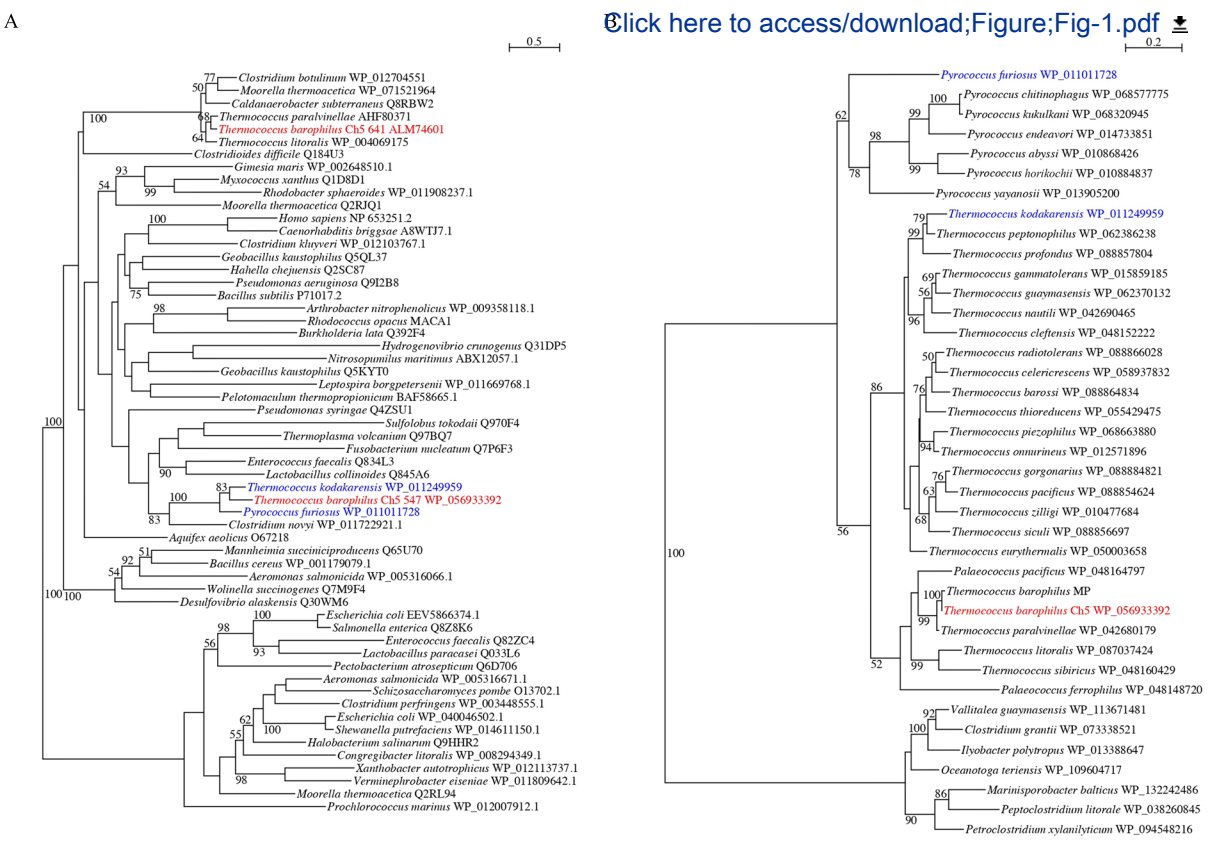

Click here to access/download;Figure;Fig-2.pdf

```
Tba_ADH547  .................MQFFSLKTRIVL..GEGSLSYIKSVAKKHSR.......VLIFSSKSMRVHGFLNETMNKVFDANAFVEAITGVPAFIEEVVE   74
Tan_ADH     ...................MFQLKTRIIE..GEGSLKALSREVRGYER.......VLILSSSSMKRHGFLGEVEDCVREAGAEVFSVTNLPAEFGVETVE   72
Tth_ADH     ...................MFWLKTRIIE..GEGSLSRLSREVKGHER.......VLILASGSMKRHGFLSEAEDYVKEAGAEVFSIAGLPAEFSVEVIE   72
Tko_ADH1    ...................MFWLKTRISE..GEDSLESLKDEAKDHER.......VLILASGSMKRHGFLSEAEDYVREAGAEVMSISGLPAEFSVEVIE   72
Tba_ADH641  ........MLWESQIPINQIFEMRCKTTNYFGVGAINKFYDIAKDLKE.RGITKVILVTGRSSYKKCGAWDVVKPALEENGIEYVHYDKIGPNFTVDMVD   91
Tpa_ADH     ........MLWESQIPINQIFELRCRTIDYFGVGAINKFYDIAKDLKENRGISRVILVTGKSSYKKCGAWDVVKPALEENGIEYVHYDKVGPNFTVDMVD   92
Thy_ADH     ........MVWESHVSINQVFEMRCKTTNYFGLCAIHKFNDIVRELKG.KGVDKVILVTGXSSYKKCGAWDVVRPALEENGVEYVHYDKVGANFTVDMID   91
Tsp_ADH     ........MVWESHVPINQVFELRCKTTDYFGLCAIHKFNGFVRELKG.KGVDRVILVTGSSSYKKCGAWDVVRPALEENGVEYVHYDKVGANFTVDMID   91
Tli_ADH     ........MLWESRLPINQVFELRCRTIDYFGVGAINKFYDIAKDLKENRDIDKVLLVTGKSSYKKCGAWDVIKPALEKYGIEYVHYDKVGPNFTVDMID   92
Tko_ADH2    MAGQSFDLNFWHPSFFLPFLQNLCDSSNKNFGRKRLPELLER.HGLSG.....KALMVTGRSSTKKTGLLYRVQELLKKAGVESIVFDRVIPNFISTHVD   94
Pfu_ADH     .........MFEISIYLP..TEIVFGPGK...LEMLPKLVKK.HGLSG.....KALIVTGRRSTKETGVLYRVQELLKQAGVESIVFDKIIPNFISTHVD   80
Zmo_ADH     ..................MASST.FYIPFVNEMGEGSLEKAIKDLNGSGF.....KNALIVSDAFMNKSGVVKQVADLLKAQGINSAVYDGVMPNFTVTAVL   78
Sce_ADH     ..................MSSVTGFYIPPISFFGEGALEETADYIKNKDY.....KKALIVTDPGIAAIGLSGRVQKMLEERGLNVAIYDKTQPNFNIANVT   79
Consensus                                                           g                   p
      an
                                I
Tba_ADH547  SIMPKVR.EFQPDLIVALGGGSVIDVAKAVKVFYDAPELKFEEVAFISRFEKPKFIPKLKTPLIAIPSTSGAGSEVSAASVLKKGDIKYN..LVSFEIAP   171
Tan_ADH     ELLPKLREEFQPDLLVALGGGSVIDTAKALKVFYDAPEVKFEEIAFIDRFSKPKFVPKLKTPLIAIPSTSGAGSEVSASSVLKKGEVKYN..IVSLEIAP   170
Tth_ADH     EFLPKVR.EFGPDLLVAMGGGSVIDTTKALKVFYDAPELNFGEIAFIDRFSKPKFVPRLKTLLIAIPSTSGAGSEVSGASVLKKGGVKYN..IVTPEIAP   169
Tko_ADH1    EFLPKVR.EFGPDLLIAMGGGSVIDTTKALKVFYDAPELVFEEIAFINRFSRPKFVPKLKTPLIAIPSTSGAGSEVSAASVLKKNGIKYN..IVTPEIAP   169
Tba_ADH641  EAAQMGR.EFGAQAVIGIGGGSPIDSAKGVAILLEYTDKDARQLYELK......FTPKKAKPVIAINTTHGTGTEVDRFAVASILEKEYKPAIAYDCIYP   184
Tpa_ADH     EAAQMGK.EFGAQAVIGIGGGSPIDTAKSVAILLEYTDKTARELYKLQ......FSPRKAKPIIAINTTHGTGTEVNRFAVASILEEEYKPAIAYDCIYP   185
Thy_ADH     EAAEMGR.EFGAQAVIGIGGGSPIDSAKSVAILLEYPDKTARDLYEFR......FTPVKAKPIIAINTTHGTGTEVDRFAVASIPEKEYKPAIAYDCIYP   184
Tsp_ADH     EAAEMGR.EFGAQAVIGIGGGSPIDSAKSVAILLEYPDKTARDLYEFR......FTPVKAKPVIAINTTHGAGTEVDRFAVATIPEKEYKPAIAYDCIYP   184
Tli_ADH     EAKEMGV.EFGAQAVIGIGGGSPIDTAKSVAILLEYPDKTGKDLYEFK......FKPTKAKPIIAINTTHGTGTEVDRFAVASILEKEYKPAIAYDFIYP   185
Tko_ADH2    EAAELAR.RENVDFVVGLGGGSAIDSAKAIAMTAKSGGKYWDYVPAVGGG....FKPSGALPIVAIPTTHGTGTEADPYAVITNPETKEKQGIGYDVLFP   189
Pfu_ADH     EGAEIAR.KENVSFVVGLGGGSAIDSAKAIAMTAASGGKYWDYVPAVGGG....FKPTGALPIVAIPTTHGTGTEADPYAVITNPETKEKQGIGYDVLFP   175
Zmo_ADH     EGLKILK.DNNSDFVISLGGGSPHDCAKAIALVATNGGEVKDYEGIDK.......SKKPALPLMSINTTAGTASEMTRFCIITDEVRHVKMAIVDRHVTP   170
Sce_ADH     AGLKVLK.EQNSEIVVSIGGGSAHDNAKAIALLATNGGEIGDYEGVNQ.......SKKAALPLFAINTTAGTASEMTRFTIISNEEKKIKMAIIDNNVTP   171
Consensus                   gggs  d  k                          i  t g   e                                    p
                                   II                                                                  III
                                   * *                                                                 * *
Tba_ADH547  EFAILDPRLPRTMPKEVARNSGLDVLVHGIEAYTTTAATPFSDAMAIKAIKLVYKWLPLSVQG..DEKARENVHYAATMAGIAFLNARLGLCHSLSHKAA   269
Tan_ADH     EVAILDPRLPRTMPGEVARNSGLDVLVHGIEAYTTKAANPFSDTMAINAIKTVYRWLPLSVKG..DEEARARVHYAATMAGIAFLNARLGLCHAMSHKAA   268
Tth_ADH     DVAILDPRLPRTMPPEVARNSGLDVLVHGIEAYTTKVASPFSDAMAIKAIKTVYRWLPLSVKG..DEEARARVHYAATMAGIAFLNARLGLCHAMSHKAA   267
Tko_ADH1    EVAILDPRLPRTMPREVARNSGLDVLVHGIEAYTTKVAGPFSDAMAIRAIKTVFEWLPKSVEG..DPEARARMHYAATMAGIAFLNARLGLAHAMSHKAA   267
Tba_ADH641  LYAIDDPALTVKLPADQTRYVTIDALNHVNEAATTKVASPYSILLAQETARLIFKYLPEALNHPDNLQAREYLLYASAIAGISFDNGLLHFTHALEHPLS   284
Tpa_ADH     LYSIDDPTLMTKLPADQTRYVTIDALNHVNEAATTKVASPYSILLAKETARLIFIYLPEALIHPDNLQAKYYLLYASAIAGISFDNGLLHFTHALEHPLS   285
Thy_ADH     LYAIDDPALTTKLPPEQTLYVTIDALNHITEAATTKVANPYSILLAKEAARLIFIYLPEALNHPDNLQARYALLYASAIAGISFDNGLLHFTHALEHPLS   284
Tsp_ADH     LYAIDDPSLTVKLSPEQTLYLTIDALNHVTEAATTKLANPYSILLAKEAARLIFIYLPEALKHPDNLQARYALLYASAIAGISFDNGLLHFTHALEHPLS   284
Tli_ADH     LYAIDDPALMTKLPANQTRYVTIDALNHVNEAATTKATNPYSILLAQETVRLISKYLPAALAHPENLQARYYLLYASAIAGISFDNGLLHFTHALEHPLS   285
Tko_ADH2    KFSIVDPEVMVTLPQNQTVYTSMDAFYHSIEAFLNVRAQPYSDVLALDSMRRVVIYLPIAYENLQDLEARTQLAWASTEAGITETLTGVIANHALEHGLS   289
Pfu_ADH     KFSIVDPELMLTLPKDQTVYTSMDAFYHSIEAFLNVRANPYSDVLALDSMRRIVIYLPLAYENLRNLEARTQLAWASTEAGITETVTGVVANHALEHGLS   275
Zmo_ADH     MVSVNDPLLMVGMPKGLTAATGMDALTHAFEAYSSTAATPITDACALKAASMIAKNLKTACDNGKDMPAREAMAYAQFLAGMAFNNASLGYVHAMAHQLG   270
Sce_ADH     AVAVNDPSTMFGLPPALTAATGLDALTHCIEAYVSTASNPITDACALKGIDLINESLVAAYKDGKDKKARTDMCYAEYLAGMAFNNASLGYVHALAHQLG   271
Consensus        dp                 d  h  ea       p     a          l          a      a   ag           h   h

                    *
Tba_ADH547  WIA...PHGLLNAIFLPYVMEFN..MRSEYARKRYAEIARELG....FNTAQELIEVIREFNEMLGVPK.LSELVSEEEFLSKLDEMSEK.AYHDPLINF   358
Tan_ADH     WIG...PHGLLNAIFIPYVMEFNA.ERSEYARKRYAEIARELG....FNTAKDLIEVVKELNEMLGVPG.LSELVDEEAFVSKVEEMANK.AYRDGLIPF   358
Tth_ADH     WIG...PHGLLNAVFLPYVMEFNA.SKSDYARRRYAEIARELG....FQTAKDLIEVVKELNEMLGVPK.LGELVDEETFASKVEEMAEK.TYHDGLIAF   357
Tko_ADH1    WVG...PHGLLNAIFIPYVMEFNA.ERSEYARKRYAEIARELG....LKSAEELIKAVRELNERLGVPK.LSELVDEETFVERVEEMAEK.AYRDGLIAF   357
Tba_ADH641  AVKPELPHGLGLAMLLPAVIKHIYPATAPILAEVYRPLVPDAKG.VPG.EALKVAKAVEKWLFSIGITEKLTDVGFGEDDVKKLAELAMTTPSLDLLLSL   382
Tpa_ADH     AVKPDLPHGLGLAILLPAVIKHIYPATARILAEIYRPLVPEVKG.VPG.EAELVAKKVEEWLFAIGITQKLTDVGFSEDDVKRLTELAMTTPSLNLLLSL   383
Thy_ADH     AVKPDLPHGLGLAMLLPAVIRQIYPATAKILAEVYRPLVPEAKG.VPG.EVELVARRVEEWLFSIGITEKLADVGFTEGDVDKLTQLAMTTPSLDLLLSM   382
Tsp_ADH     AVKPDFPHGIGLAMLLPAVIRHIYPATAKILAEVYRPLVPEAKG.VPG.EVELVARRVEEWLFSIGITEKLEDVGFSETDVNRLTELAMKTPSLNLLLSM   382
Tli_ADH     AVKPDLPHGLGLAMLLPAVVKHIYPATAEILAEVYRPIAPEAKG.YPG.EAEFVAKRIEQWLFSIGIKEKLTDVGFGEDDIDKLTKLAMETPGLDGLLAM   383
Tko_ADH2    GFYPEVPHGLGLCILGPYLFEYILDHAYERLAIVGREVFGVYES.NDRKAAELAVKKLRDFQSLFGVNKKLRELGVKEEDIPKMAETAYR..MMKGVIDV   386
Pfu_ADH     GFYPEVPHGLGLCILGPYLFEYILDYAYEKLAIVGREVFGVYEP.NDRKAAELAIKKLRDFQSLFGVNKKLRELGVKEEDIPEMARTAYR..MMKPVIEA   372
Zmo_ADH     GYY.NLPHGVCNAVLLPHVLAYNASVVAGRLKDVGVAMGLDIANLGDKEGAEATIQAVRDLAASIGIPANLTELGAKKEDVPLLADHALK....DACALT   365
Sce_ADH     GFY.HLPHGVCNAVLLPHVQEANMQCPKAKKRLDEIALHFGAS....QEDPEETIKALHVLNRTMNIPRNLKELGVKTEDFEILAEHAMH....DACHLT   362
Consensus        phg       p                                                                 l

Tba_ADH547  NPVEPSIEEIKELYKRAFYD...   378
Tan_ADH     NPVEPKPEEIRELYLRAFYGR..   379
Tth_ADH     NPVEPKPEEIKELYLKAYRGE..   378
Tko_ADH1    NPVEPKPEEIRELYLKALNAL..   378
Tba_ADH641  APIPATKETVEAIYRDSLYPLSE   405
Tpa_ADH     APVEATKETIEAIYRDSLYPLSK   406
Thy_ADH     APVEATKERIAAIYRDSLYPIGR   405
Tsp_ADH     APGEATRERIAAIYRDSLYPISR   405
Tli_ADH     APVEANEDVIRAIYRDSLYPLSE   406
Tko_ADH2    TPGNLSVEDLEEIYRRAY.....   404
Pfu_ADH     TPGDLKVEDLEEIYRRAY.....   390
Zmo_ADH     NPRQGDQKEVEELFLSAF.....   383
Sce_ADH     NPVQFTKEQVVAIIKKAYEY...   382
Consensus    p
```

A

Click here to access/download Figur

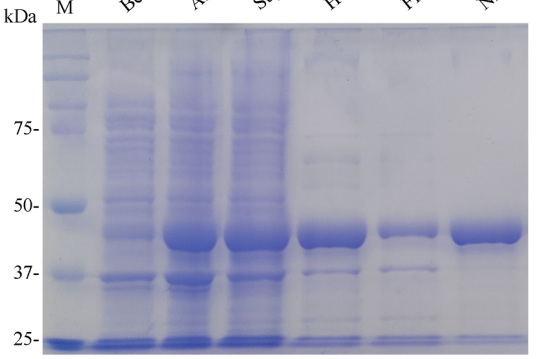

B

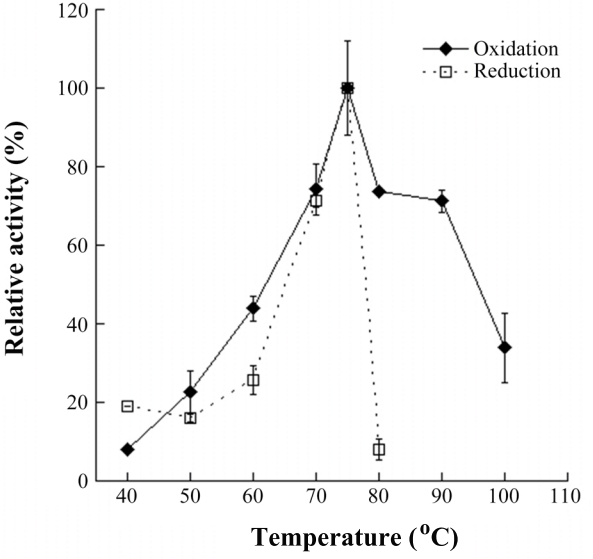

Figure

Click here to access/download;Fig

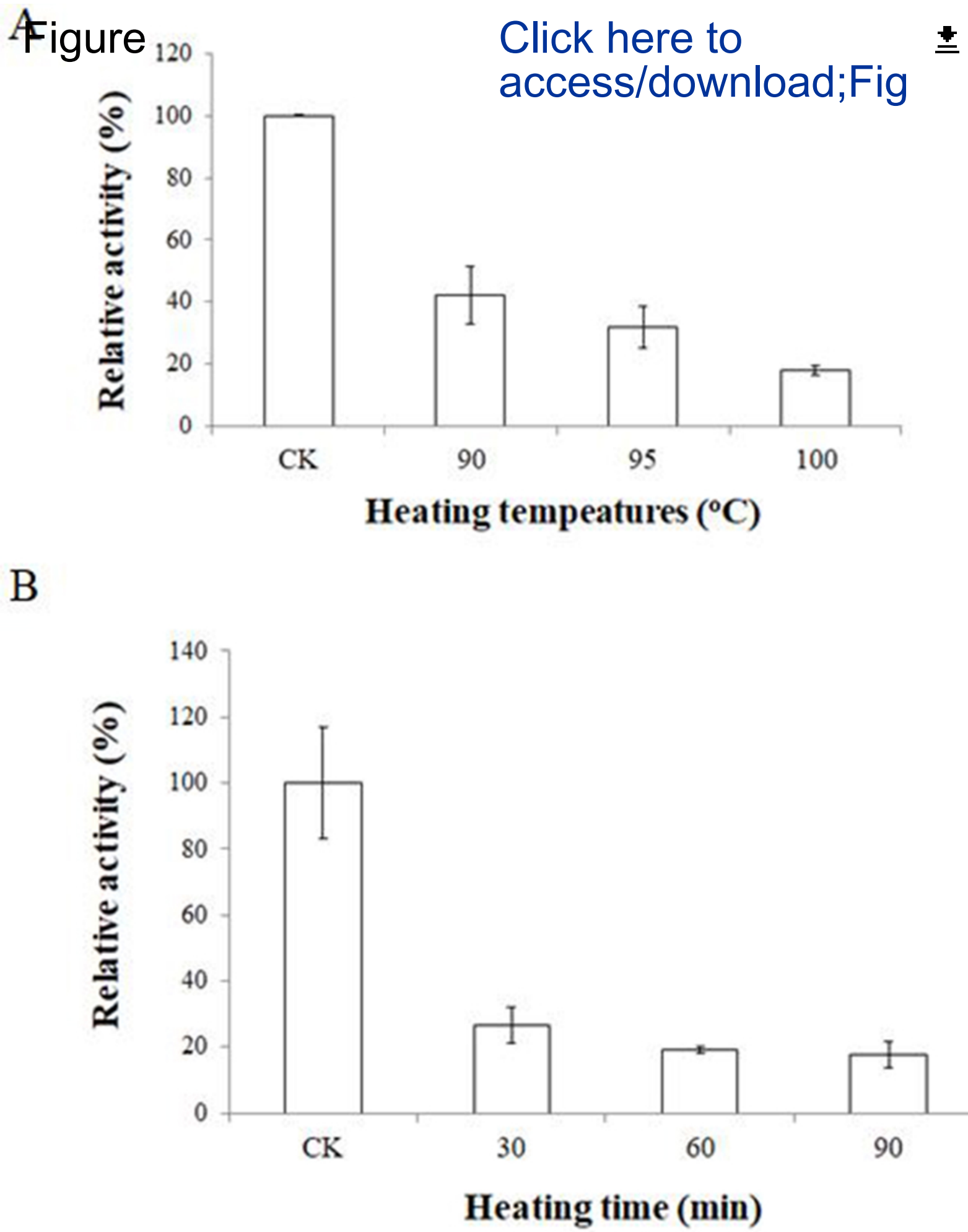

Click here to access/download:Fig

A

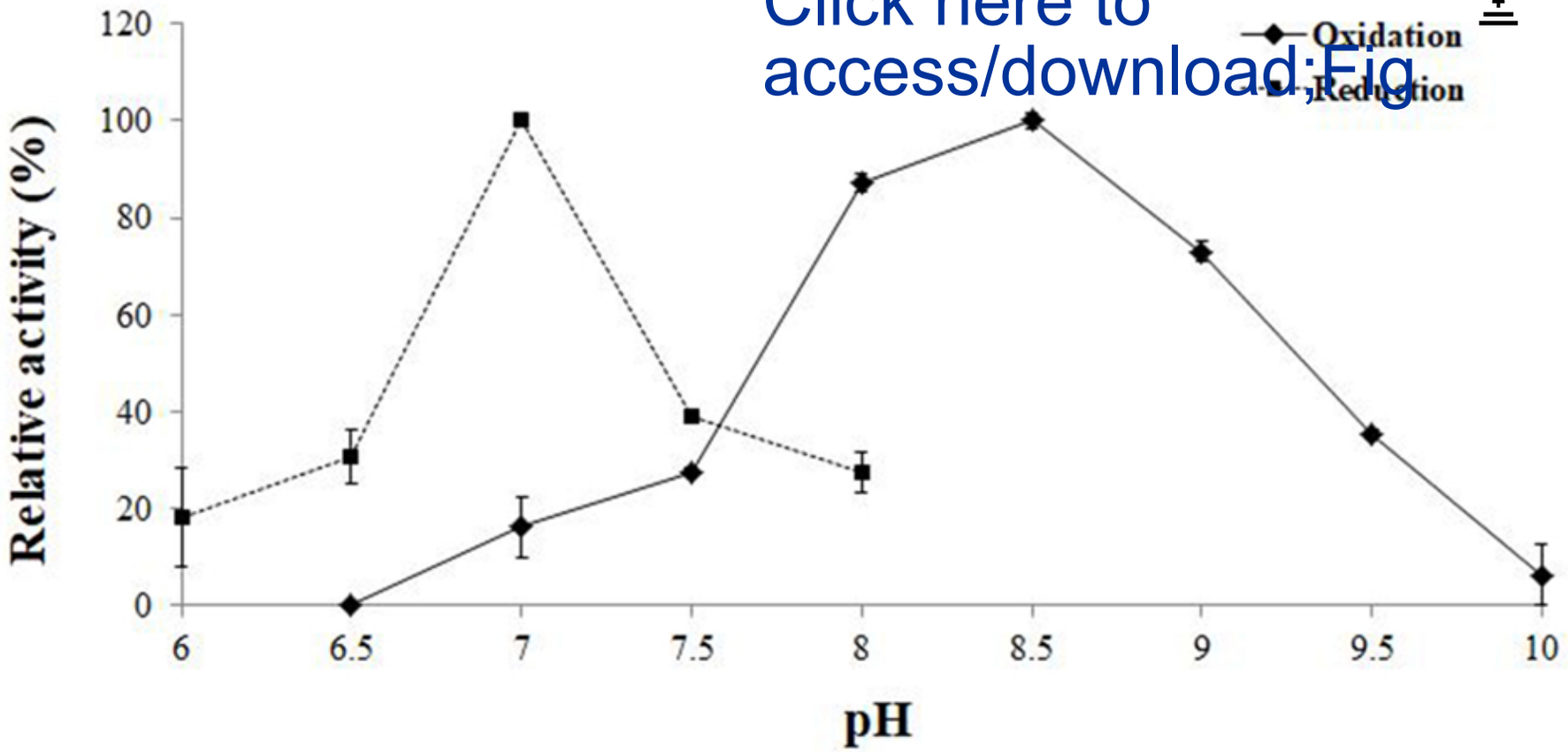

B

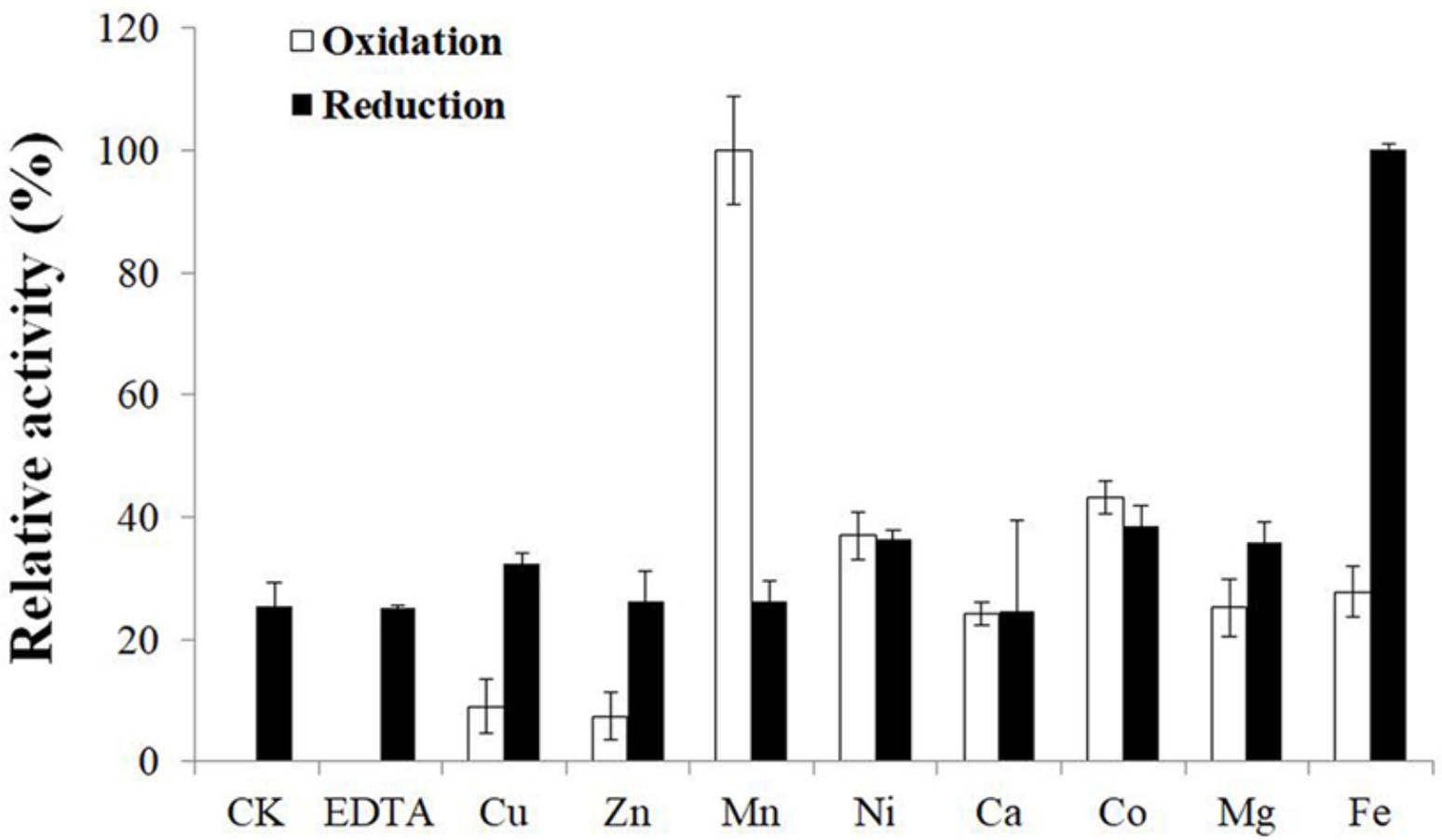

Click here to access/download;Fig

A

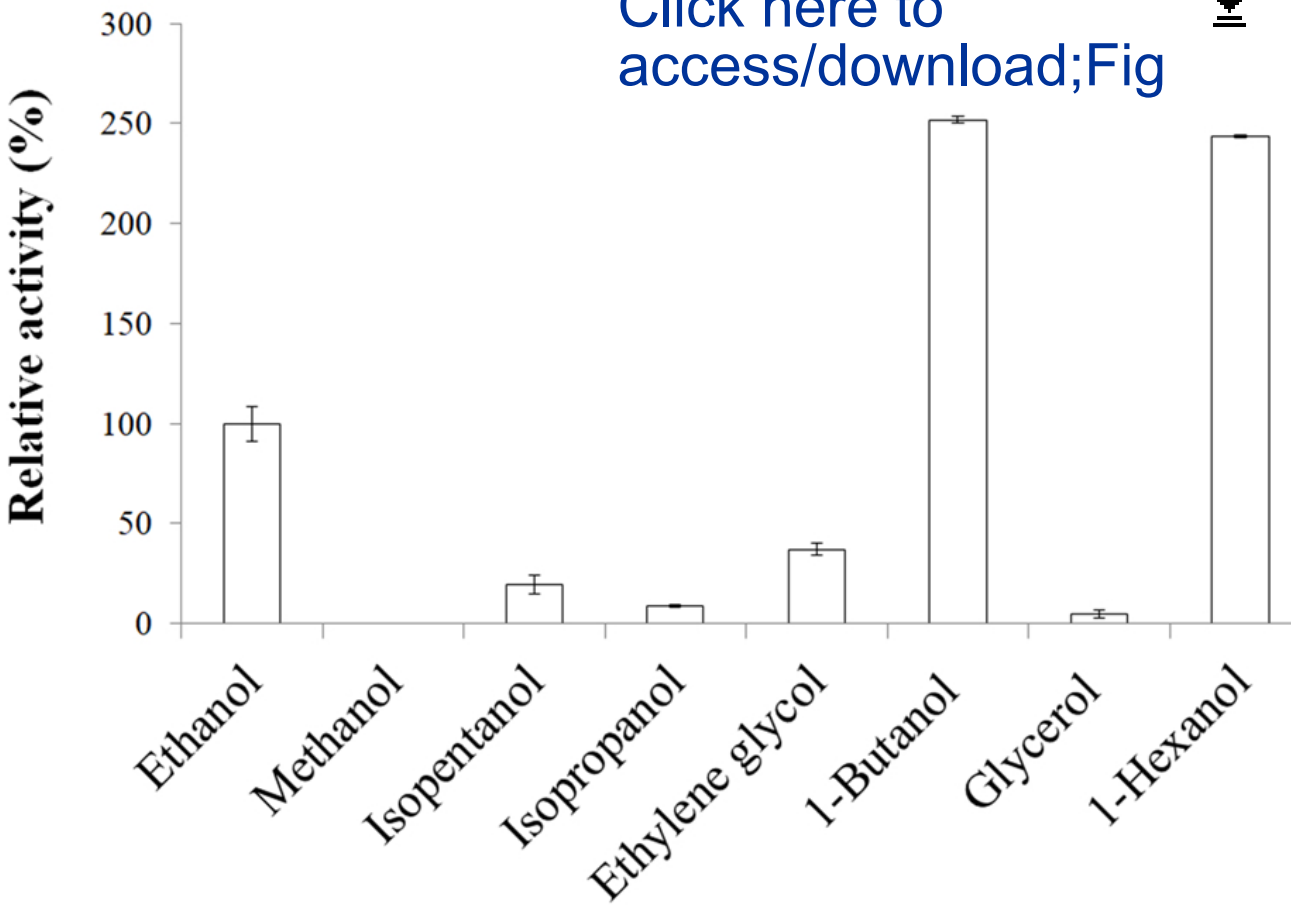

B

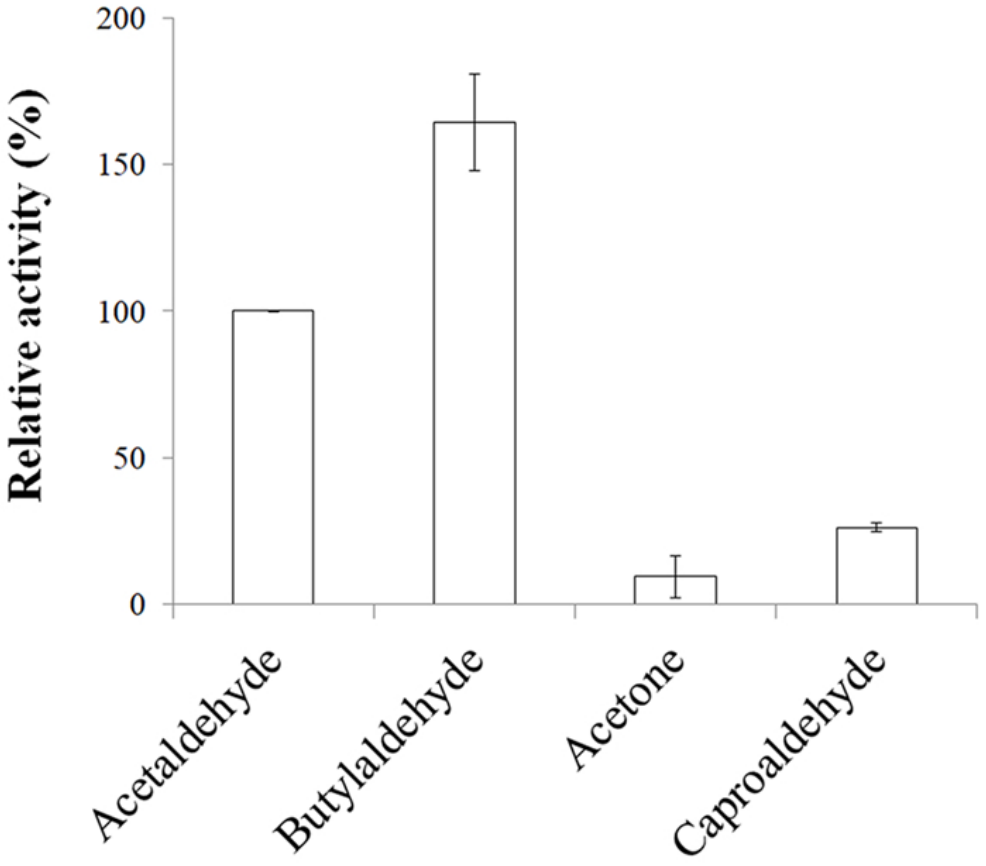

A

Click here to access/download;Figu

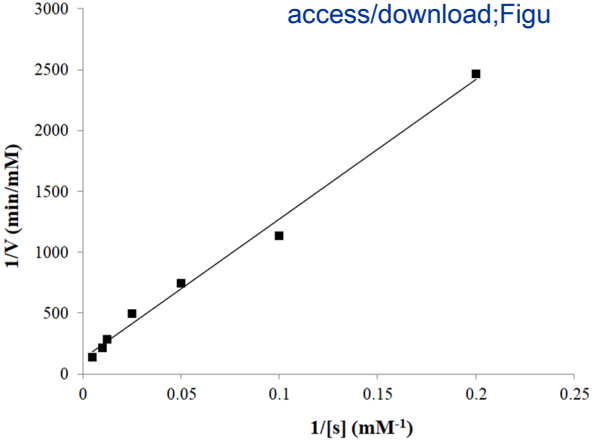

B

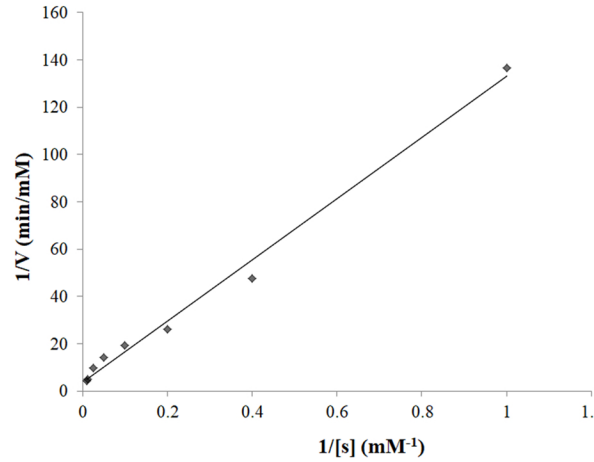

Figure

Click here to access/download;Figure;updated Fig-

A

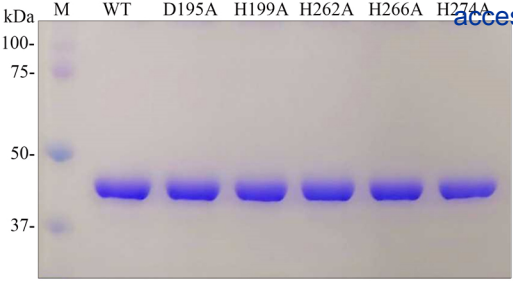

B

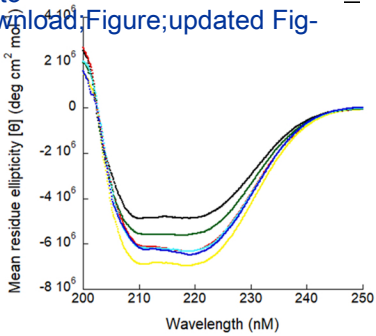

C